Grant agreement no. 667510

GLINT

Research and Innovation Action
H2020-PHC-2015-two-stage

D4.3 Assessment of GlucoCEST effect of 3OMG on a number of tumour models including from breast tumour cell lines DA3, 4T1, and MCF7 and brain metastases of the DA3 tumour cells

Work Package:	4
Due date of deliverable:	31/12/2018
Actual submission date:	8/1/2019
Lead beneficiary:	TAU
Contributors:	Michal Rivlin
Reviewers:	UCL, UNITO

Project co-funded by the European Commission within the H2020 Programme (2014-2020)		
Dissemination Level		
PU	Public	YES
CO	Confidential, only for members of the consortium (including the Commission Services)	
CI	Classified, as referred to in Commission Decision 2001/844/EC	

*"This project has received funding from the European Union's Horizon 2020 research and innovation programme under the Grant Agreement No **667510**"*

Disclaimer

The content of this deliverable does not reflect the official opinion of the European Union. Responsibility for the information and views expressed herein lies entirely with the author(s).

*"This project has received funding from the European Union's Horizon 2020 research and innovation programme under the Grant Agreement No **667510**"*

Contents

*"This project has received funding from the European Union's Horizon 2020 research and innovation programme under the Grant Agreement No **667510**"*

1 Version log

Version	Date	Released by	Nature of Change
V1.0	11/12/2018	M. Rivlin	First version
V1.1	23/12/2018	M. Rivlin	Revised
V1.2	13/03/2019	M. Rivlin	Revised

*"This project has received funding from the European Union's Horizon 2020 research and innovation programme under the Grant Agreement No **667510**"*

2 Objectives

The objective of this deliverable is to test the ability of CEST MRI of 3OMG to detect tumours in several breast cancer models of murine and human origin, for different routes of administration of 3OMG and to compare the method with glucoCEST and with 18FDG-PET on the same animals.

*"This project has received funding from the European Union's Horizon 2020 research and innovation programme under the Grant Agreement No **667510**"*

3 Report on activities carried out and results

3.1 Work carried out broken down by task

- **Examination of the ability of CEST MRI of glucose and of 3-O-methyl-D-glucose (3OMG) to detect tumours in several breast cancer models of murine and human origin**

Main: The observed CEST effect in four tumours models (DA3, 4T1, MDA-MB-231 and MCF7) lasted more than an hour following per os administration of 3OMG (dose = 1.0 g/kg). The GlucoCEST contrast at 1.2 ppm (relative to the water signal) in 4T1 tumours has higher signal than that of MDA-MB-231 and MCF7 tumours.

- **Identification of the lowest detectable dose of 3OMG in breast cancer models.**

Main: In the 4T1 model, per os administration of 0.45–3.0 g/kg 3OMG increased the CEST signals in the tumours by ~2–10% relative to the baseline (by oral administration). The lowest detectable dose was examined statistically: a one-way analysis of variance to test for differences in the % CEST obtained at different 3OMG doses revealed statistically significant differences ($P < 0.00001$); Tukey's post hoc test showed the main differences to be between 7 groups of doses (0.45-3.0 g/kg). At a dose of 0.6 g/kg the level of the CEST was 4% above the baseline and the CNR for this dose was 3.9. This CNR level ensures that the signal can be quantified easily over the contribution of the background.

- **Examination of the ability of CEST MRI of 3-O-methyl-D-glucose (3OMG) to detect tumours by different routes of administration of the agent**

Main: The efficacy of different routes of 3OMG administration was examined. A total of 9 mice bearing 4T1 tumours received 3OMG via IV, IP and PO administration (for each administration route n=3) and the GlucoCEST effect obtained in the tumours was compared. For the three routes of administration, the same maximum effect was obtained, achieved at about 20min after administration.

*"This project has received funding from the European Union's Horizon 2020 research and innovation programme under the Grant Agreement No **667510**"*

- **Comparison between glucose and 3OMG to provide GlucoCEST contrast (on the same animals).**

Main: The 3OMG CEST contrast was compared to that of glucose. The same tumour bearing mice were imaged twice, with an interval of ca. 8 hours between the two administration of glucose and 3OMG. 3OMG MRI gave higher net GlucoCEST effect (4.6%) than that of D-glucose (2.7%) even at half of the dosage (0.7 g/kg 3OMG vs 1.5 g/kg D-glucose). Moreover, the GlucoCEST contrast arising upon glucose injection lasted only for a short time and was reduced to the baseline level after 40 minutes, whereas that of 3OMG persisted for more than an hour.

- **Comparison the method with 18FDG-PET (on the same animals)**

Main: When 3OMG-CEST MRI was compared with conventional scanning by 18FDGPET, they showed similar trends, as evidenced by the good agreement between the tumour uptake results of the two modalities (the percentage CEST contrast and percentage ID/mL of 18FDG uptake by the tumour)**.**

3.2 Significant results achieved

- A marked 3OMG-CEST MRI contrast that was correlated with the administrated dose was obtained in several breast cancer models
- A marked 3OMG-CEST MRI contrast that was correlated with different routes of administration.
- Identification of the lowest detectable dose of 3OMG in breast cancer models- PO administration of 570 mg/kg of 3OMG yielded 3-4% CEST above the baseline.
- 3OMG-CEST contrast reached its maximum at 20 min after administration and lasted for more than an hour, while that of glucose was lower and diminished after 20 min.
- 3OMG-CEST showed comparable results to that of FDG PET.

3.3 Expended results

A full in vivo Z spectra and MTRasym plots of 4T1 tumours before and after 3OMG administration (2–3 g/kg) are shown in Figure 1. The relatively large CEST signal at baseline (about 14% at about 1 ppm from the water signal) must be due to the presence of a variety of metabolites, such as the glycosaminoglycans and poly-sialic acid residues of mucoproteins

*"This project has received funding from the European Union's Horizon 2020 research and innovation programme under the Grant Agreement No **667510**"*

known to be abundant in many tumours. The increase of the MTRasym as a result of 3OMG treatment in the region of approximately 1 ppm (from the water signal) is clearly seen.

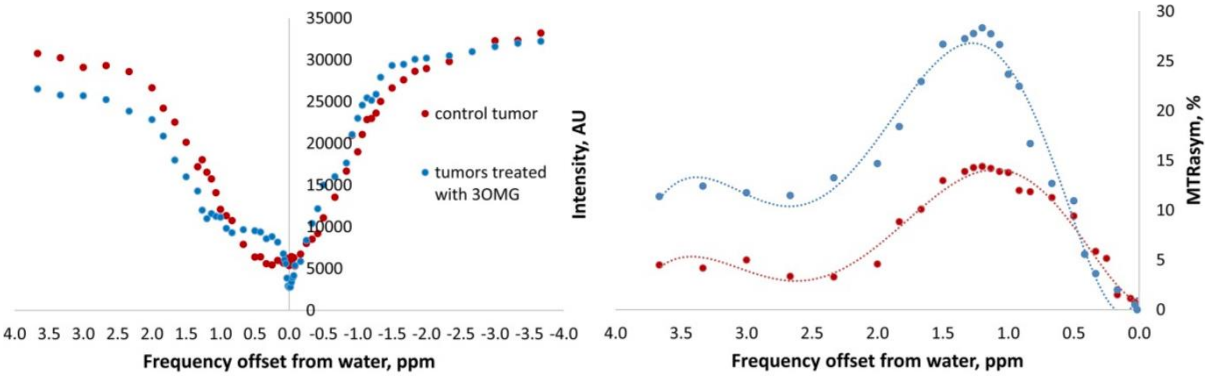

Figure 1: Z spectra (a) and MTRasym (b) plots of mice bearing 4T1 tumours with and without 3OMG treatment. (The plot of tumours treated with 3OMG represents combined results of three mice, two of them were treated with 3 g/kg of 3OMG, PO, and one was treated with 2 g/kg of 3OMG, IP).

The ability of 3OMG CEST MRI to image in vivo mammary tumours was demonstrated. We injected IP a 3OMG solution into mice bearing DA3 tumours after imaging the tumour anatomy by T2-weighted spin echo sequence (RARE). The images obtained in one of the experiments are shown in Figure 2 together with the calculated CEST values for a total of five experiments.

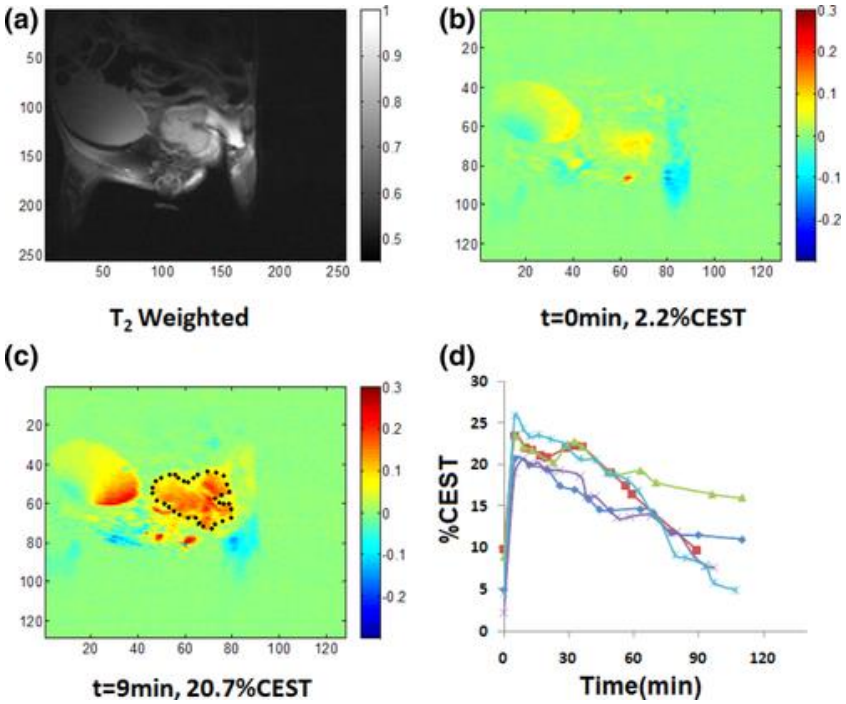

Figure 2: CEST MRI kinetic measurements in the tumour at different times following injection of 3OMG, 1.5 g/kg. (B1 = 2.5 μT, B0 = 7 T). a: A T2-weighted image before the administration of the agent. b: A CEST image before the administration of the agent. c: A CEST image 9 min

*"This project has received funding from the European Union's Horizon 2020 research and innovation programme under the Grant Agreement No **667510**"*

after the injection. The marked ROI was used for the CEST calculation. d: The time series of the %CEST for the five mice tested.

As seen in Figure 2, a strong and sharp CEST effect was visualized at the tumour within a few min of the 3OMG injection (1.5 g/kg), and reached 20% above the control at 9 min. With the exception of the urinary bladder no other organs showed a significant CEST effect on the MRI scans session. The enhanced CEST declined slowly reaching half its maximum value after approximately 80 min. These results were replicated in five experiments with initial CEST enhancement of 20.7 ± 1.6%.

Representative T2-weighted anatomical images and the 3OMG-CEST contrast of 4T1, MDA-MB-231 and MCF7 breast tumours are shown in Figure 3. While the T2-weighted images exhibited only the morphology pattern (Figs. 3a,d,g), CEST MRI following 3OMG administration produced clear patterns of the tumours that reflected their metabolic activity and clearly distinguished them from other parts of the body in the three tested models (Figs. 3c,f,i). The CEST effect of the three tumours models lasted more than an hour following PO administration of 1.0 g/kg 3OMG. Figures 3j,k show the higher signal (P = 0.009) of the CEST contrast at 1.2 ppm (relative to the water signal) of the 4T1 tumour compared with the signal coming from the MDA-MB-231 and MCF7 tumours.

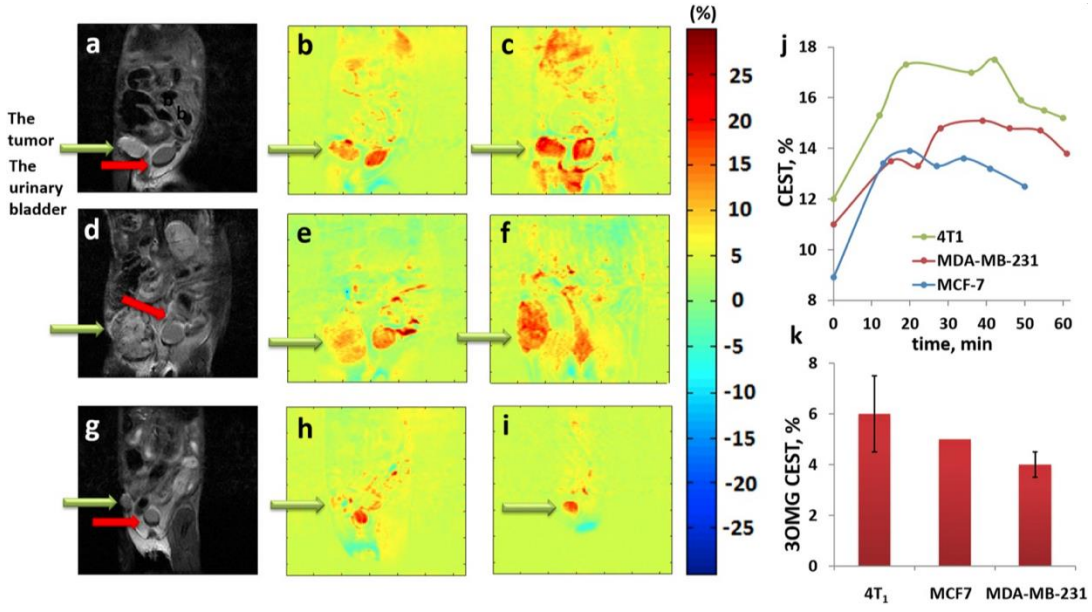

Figure 3: Imaging of three breast cancer models: 4T1 (a–c), MDA-MB-231 (d–f), and MCF-7 (g–i). a,d,g: T2-weighted images of the three models, respectively. b,e,h: CEST maps at baseline for the three models, respectively. c,f,i: CEST maps ~60 min after 3OMG administration (PO, 1.0 g/kg) for the three models, respectively. j: An example of the time

*"This project has received funding from the European Union's Horizon 2020 research and innovation programme under the Grant Agreement No **667510**"*

series of the % CEST observed in the tumours for the three models. k: A bar graph showing average 3OMG-CEST contrast ± SD, i.e., the % CEST due to 3OMG administration, for the three examined tumours: 4T1 (n = 6), MCF7 (n = 1) and MDA-MB-231 (n = 3). Green arrows point to the tumours and red arrows to the urinary bladder. The CEST was measured at a frequency offset of 1.2 ppm, B1 = 2.4 μT.

In the 4T1 model, PO administration of 0.45–3.0 g/kg 3OMG increased the CEST signals of the tumours by ~2–10% relative to the baseline (Fig. 4d). A one-way analysis of variance to test for differences in the % CEST obtained at different 3OMG doses revealed statistically significant differences ($P < 0.00001$); Tukey's post hoc test showed the main differences to be between 7 groups of doses. At a dose of 0.6 g/kg the level of the CEST was 4% above the baseline (Fig. 4d) and the CNR for this dose was 3.9 (Table 1). This CNR level ensures that the signal can be quantified easily over the contribution of the background.

Figures 4a–c present an experiment with a necrotic area at the center of the tumour. The difference between the CEST images (Figs. 4b,c) can be ascribed to the trapped agent (3OMG) in the tumour. As can be seen in Figure 4c, the CEST effect was most pronounced at the rim of the tumour, presumably the most metabolically active part.

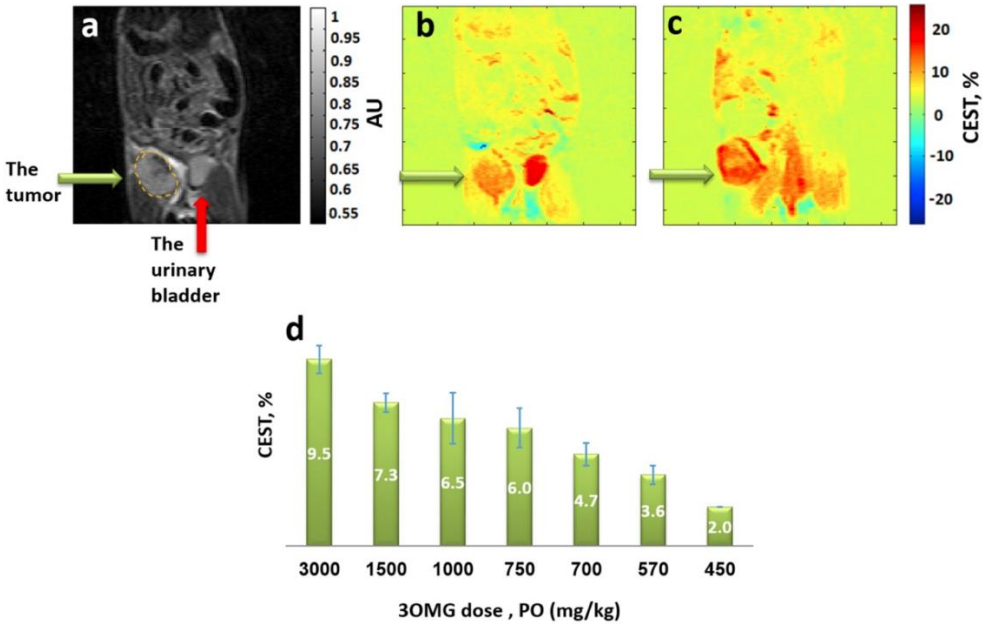

Figure 4: Dose dependence of 3OMG-CEST MRI for mice bearing 4T1 breast tumours at a frequency offset of 1.2 ppm, B1 = 2.4 μT. a: A T2-weighted image before administration of the agent. b: A CEST image before administration of the agent; 12% CEST was obtained in the tumour. c: A CEST image 80 min after PO treatment with 3OMG, 0.6 g/kg; 16.4% CEST was obtained in the tumour. The marked ROI in (a) was used for the CEST calculation. Green arrows point to the tumour and the red arrow to the urinary bladder. d: Bar graph showing mean ± SD of 3OMG-CEST contrast one hour after 3OMG administration (n = 24).

*"This project has received funding from the European Union's Horizon 2020 research and innovation programme under the Grant Agreement No **667510**"*

Table 1: Quantitative Comparison of 3OMG Dose versus the Measured CNR of the CEST Map

3OMG dose (mg/kg)	Mean of CEST map (baseline)	STD noise (baseline)	Mean of CEST map (treatment)	STD noise (treatment)	Contrast of CEST map (treatment-baseline)	CNR
450	0.111	0.0054	0.130	0.0068	0.019	2.19
570	0.120	0.0071	0.156	0.0058	0.036	3.93
700	0.098	0.0049	0.145	0.0045	0.047	7.06
750	0.098	0.0053	0.158	0.0056	0.06	7.78
1000	0.110	0.0051	0.175	0.0039	0.065	10.12
1500	0.130	0.0062	0.203	0.0047	0.073	9.38
3000	0.125	0.0057	0.221	0.0059	0.096	11.70

The 3OMG-CEST method was compared with the glucoCEST method (Fig. 5) in a side by side experiment in the same animal, with an interval of ~8 h between the two methods. 3OMG-CEST MRI gave a higher CEST effect than D-glucose, even at half the dose used for the latter (0.7 g/kg 3OMG versus 1.5 g/kg D-glucose). Moreover, the 3OMG-CEST effect persisted for more than an hour while the glucoCEST effect lasted only a short time and fell to baseline after 40 min

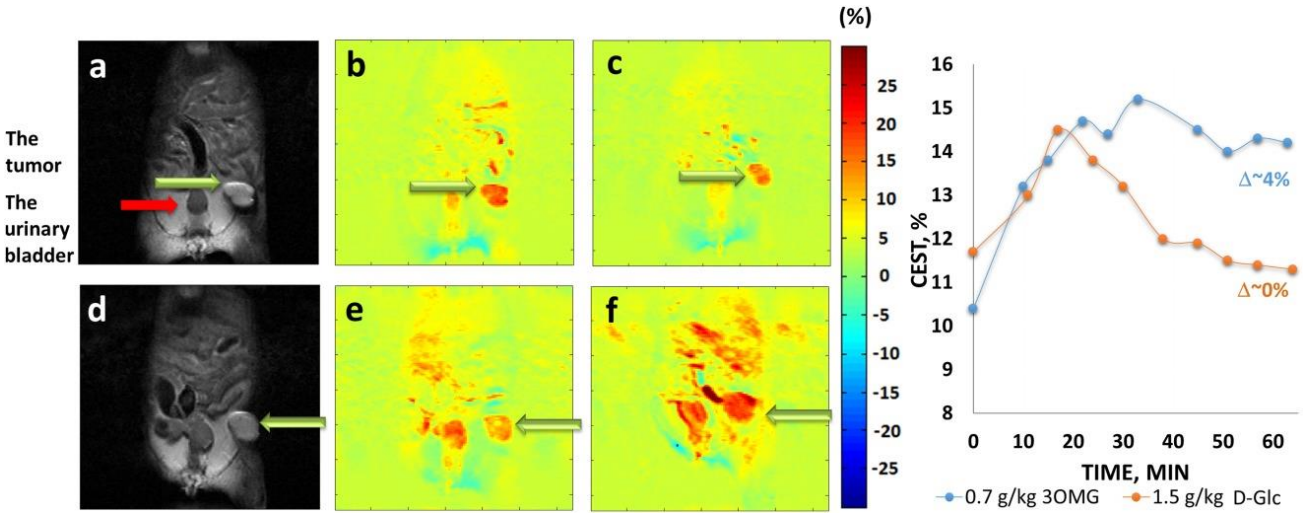

*"This project has received funding from the European Union's Horizon 2020 research and innovation programme under the Grant Agreement No **667510**"*

Figure 5: 3OMG-CEST versus glucoCEST MRI kinetics measurements in 4T1 breast tumour model in the same animal. a: An anatomical T2-weighted image before D-glucose administration. b,c: CEST map before (b) and ~60 min after (c) PO treatment with D-glucose, 1.5 g/kg (at frequency offset of 1.2 ppm, B1 = 2.4 μT). No remarkable CEST contrast was obtained in the tumour vis-a-vis the baseline. d: An anatomical T2-weighted image before 3OMG administration. e,f: CEST map before (e) and ~60 min after (f) PO treatment with 3OMG, 0.7 g/kg (at frequency offset of 1.2 ppm, B1 = 2.4 μT). Approximately 4% CEST was obtained in the tumour with reference to the baseline. Green arrows point to the tumour, the red arrow to the urinary bladder. g: The time series of the % CEST achieved in 4T1 tumour following treatment with D-glucose (1.5 g/kg) versus 3OMG (0.7 g/kg).

In vitro experiments were performed to compare the CEST effect obtained from D-glucose and 3OMG phantom solutions consisting of 20 mM of these metabolites. To have T1 and T2relaxation times of the phantoms to be comparable to those of the 4T1 tumours (T1 = 1100 ms, T2 = 60 ms), 0.075 mM of MnCl2 was added. After the addition of 0.075 mM of MnCl2 the T1 and T2 values were 950 ms and 84 ms for 3OMG solution and 1000 ms and 87 ms D-glucose solution, respectively. The MTRasym at frequency offset of 1.2 ppm from the water signal point to 11.5% versus 5.5% for the 3OMG versus D-glucose solution (at T = 37 °C and pH = 7.4, at the 7T magnetic field).

In this study, the % of CEST obtained with different modes of administration (IV, IP, and PO, n=3 for each mode) of 3OMG were compared in nine mice bearing 4T1 tumours. The three modes produced nearly identical maximum effect approximately 20 min after treatment (Fig. 6).

*"This project has received funding from the European Union's Horizon 2020 research and innovation programme under the Grant Agreement No **667510**"*

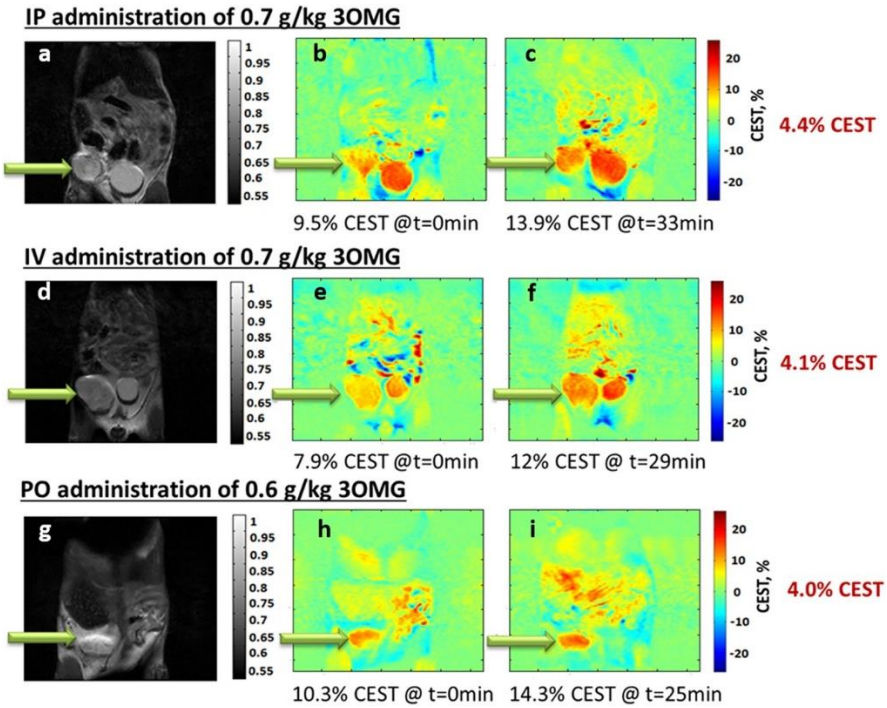

Figure 6: Mice bearing 4T1 tumours received 3OMG by means of IP, IV, and PO administration and the % CEST obtained in the tumours was compared. a,d,g: An anatomical T2-weighted image before 3OMG administration. b,e,h: CEST map before treatment. c,f,i: CEST map after treatment with 3OMG. Green arrows point to the tumours.

3OMG-CEST MRI was compared with FDG PET/CT by testing the two techniques on the same six mice carrying 4T1 tumours (Fig. 7). In the CEST MRI experiments, images were acquired from a coronal slice of each tumour at baseline and for 60 min after PO treatment with 3OMG. The images revealed a significant CEST contrast in the tumours (8 days after 4T1 cells injection). Moreover, significant CEST signal was observed in the area of the liver. 4T1 tumours are known to metastasize from the primary tumour in the mammary gland to multiple distant sites including blood, lungs and the liver. Two to 3 days after the MRI scans, the mice were administered 18FDG for PET/CT evaluation. The PET/CT was performed on tumour slices corresponding to the MR imaging slices. In agreement with the 3OMG-CEST MRI experiments, the activity at 60 min after 18FDG administration was significantly higher in the tumours and the urinary bladders. Significant 18FDG accumulation could also be seen at the liver, presumably due to metastasis. The results point to a correlation between the 3OMG-CEST contrast and the FDG uptake of the tumours, providing clear validation of the 3OMG-CEST technique.

*"This project has received funding from the European Union's Horizon 2020 research and innovation programme under the Grant Agreement No **667510**"*

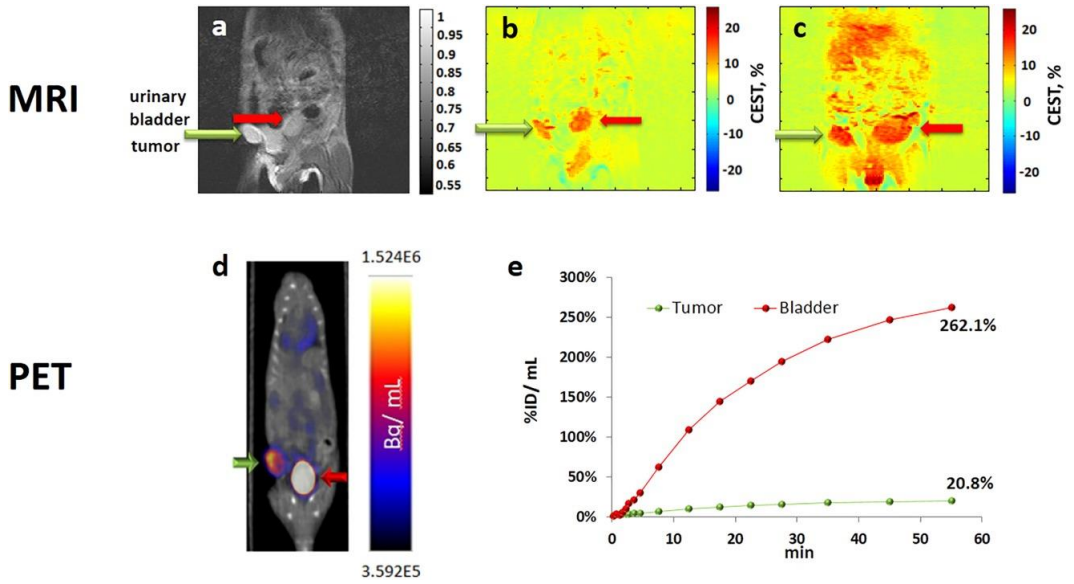

Figure 7: 3OMG-CEST MRI and 18FDG PET/CT images from a 4T1 tumour in the same mouse. a: A coronal view of an anatomical T2-weighted MR image before 3OMG administration showing the tumour (green arrow) and the urinary bladder (red arrow). b: A CEST image before administration of the agent (at frequency offset of 1.2 ppm, B1 = 2.4 μT). c: A CEST image 60 min after PO treatment with 3OMG, 1.0 g/kg (at frequency offset of 1.2 ppm, B1 = 2.4 μT); 7% CEST was obtained in the tumour, higher than the baseline, and significant CEST contrast was obtained also in the urinary bladder and areas suspected to be metastases. d: 18FDG PET/CT coronal view obtained 60 min after IV injection of 18FDG showing accumulation mainly in the tumour (green arrow) and urinary bladder (red arrow). e: The time series of the % ID/mL 18FDG uptake in the tumour and urinary bladder. The CEST and PET/CT experiments were run 8 and 10 days after implantation of the tumour, respectively.

For further details, see reference (1).

3.4 Deviation

While GlucoCEST effect/signal of 3OMG was demonstrated with several tumour models (DA3, 4T1, MCF7 and even with MDA-MB-231 model that wasn't included in the task), brain metastasis of DA3 cell line were not identified. As it is challenging to predict which animal will develop brain metastasis and whether they will survive the experiment in this state, for future research we suggest examining the efficacy of the method for a model of brain tumour that mimics glioblastoma. This deviation will not diminish from the overall results of the project, after all, GlucoCEST effect was already demonstrated on several models and in several lab study, and we have shown the presence of metastasis in the liver and lung by glucoCEST of other glucose analogue (2).

*"This project has received funding from the European Union's Horizon 2020 research and innovation programme under the Grant Agreement No **667510**"*

4 Conclusions

A remarkable 3OMG-CEST MRI contrast was established in several different breast cancer models, with a) correlation to the administrated dose of 3OMG and the resultant CEST signal b) improved signal compare to glucoCEST c) comparable results to that of FDG-PET. The noninvasive 3OMG-CEST MRI method offers advantages over currently available imaging modalities for evaluation in the clinic, for detecting and monitoring the progression of tumors, and for assessing their response to therapy, all while avoiding exposing the patient to radiation. Note that the scans were performed at a high field (7T) that is not routinely used in the clinic. One problem with the CEST MRI of glucose and its derivatives is the relatively small frequency offset from the water peak that gives maximal CEST effect. So far, CEST MRI with the same frequency offset of 1.2 ppm (that used for the 3OMG CEST MRI study) was used in clinical 3T MRI scanners. One successful example is the gagCEST, based on sugar hydroxyl protons of the glycosaminoglycan, which are similar to those of the glucose-based CEST (glucoCEST). Successful results of glucoCEST were obtained with administration of glucose in human subjects. As was demonstrated in the present work 3OMG gives better CEST effect compared to glucose and the slow decay of the 3OMG CEST signal may allow enough time to perform such a procedure. Therefore, the extension of our positive results with 3OMG on mice at 7T to human 3T scanner seems very encouraging. The deliverable 4.3 was fully achieved.

*"This project has received funding from the European Union's Horizon 2020 research and innovation programme under the Grant Agreement No **667510**"*

5 Bibliography / References

1. Rivlin, M. & Navon, G. Magn Reson Med **79**, 1061-1069 (2018).
2. Rivlin, M. & Navon, G. *Scientific Reports* **6**, 32648 (2016).
3. Ling, W et al. *Pro Nat Acad Sci* **105**, 2266-2270 (2008).

*"This project has received funding from the European Union's Horizon 2020 research and innovation programme under the Grant Agreement No **667510**"*